Optical coherence computed tomography

Li Li, Lihong V. Wang

Li Li, Lihong V. Wang, "Optical coherence computed tomography," Proc. SPIE 6855, Complex Dynamics and Fluctuations in Biomedical Photonics V, 68550H (6 February 2008); doi: 10.1117/12.761431

SPIE.

Event: SPIE BiOS, 2008, San Jose, California, United States

Optical coherence computed tomography

Li Li*, Lihong V. Wang*†

*Optical Imaging Laboratory, Department of Biomedical Engineering, Washington University in Saint Louis, Saint Louis, Missouri, USA 63117.

†Email: lhwang@biomed.wustl.edu

ABSTRACT

We proposed a novel time-resolved optical tomography, optical coherence computed tomography. It married the key concepts of time-resolved diffuse optical tomography and optical coherence tomography. Both ballistic and multiple-scattered photons were measured at multiple source-detection positions by low-coherence interferometry. It measures the reemitted light with a temporal resolution of 56 femtoseconds, which is much better than the resolution of conventional time-resolved detection systems. A light-tissue interaction model was established using the time-resolved Monte Carlo method. The optical properties were then reconstructed by solving the inverse time-resolved radiative transport problem under the first Born approximation. Our initial results showed the potential of this technology to bridge the gap between diffuse optical tomography and optical coherence tomography.

Keywords: Optical coherence tomography, diffuse optical tomography, Monte Carlo, radiative transfer

1. INTRODUCTION

For biomedical applications, optical methods are safe, versatile and cost-effective. Thus, a lot of optical imaging techniques have been developed during the last decade. Among them, time-resolved techniques are known to collect the richest information, and provide high-quality map of tissues' optical properties as a result. Here, we present a novel time-resolved optical imaging modality referred to as optical coherence computed tomography (optical CCT). Optical CCT[1] marries the key concepts of the two most popular optical tomographical techniques—diffuse optical tomography (DOT)[2,3] and optical coherence tomography (OCT)[4,5]. We demonstrated with our preliminary experiment results that optical CCT was a promising candidate to bridge the gap between DOT and OCT.

DOT works in the diffusive regime. It measures the reemitted light from tissue through a large number of source-detection pairs. Also, a model, usually based on diffusion theory, is adopted to predict the photon migration in tissues. Finally, maps of tissues' optical properties are achieved by matching the predictions from this model and experimental measurements, generally through an iterative procedure. DOT can image a few centimeters into tissue when using near-infrared light. However, the spatial resolution is poor, typically about 1/5 of the imaged depth. This is due to the nature of photon diffusion. The time-domain DOT measures the delayed and broadened temporal profiles of an ultra-short light pulse after traveling through a medium. It is expected to outperform its continuous-wave and frequency-domain counterparts since it carries information of a broad spectrum simultaneously. Traditionally, the temporal profiles of reemitted light were measured by sophisticated high-sensitivity detection systems, such as a streak camera[6] and a time-correlated single-photon counting system[7]. However, the slow frame-rate and the high cost limited their application. Recently, time-gated optical image intensifier[8] has been utilized to

Complex Dynamics and Fluctuations in Biomedical Photonics V, edited by Valery V. Tuchin, Lihong V. Wang,
Proc. of SPIE Vol. 6855, 68550H, (2008) · 1605-7422/08/$18 · doi: 10.1117/12.761431

develop fast parallel time-resolved DOT. However, the gate width is usually ~200 ps, corresponding to a pathlength as long as 6 cm in air. A finer temporal resolution is preferred to resolve biological structure better, especially for applications in small-animal models.

In this paper, we propose to make time-resolved measurements of multiple-scattered photons as well as ballistic ones using low-coherence interferometry. Temporal resolution finer than 100 fs can be easily achieved using ordinary low-coherence sources, such as a superluminescent diode, a femtosecond laser, or a wavelength-swept laser. This method has high sensitivity (generally better than 90 dB) due to the amplification of signal by a strong reference signal. Also, it can provide a wide dynamic range because the interference signal is proportional to the amplitude, instead of the intensity, of the light remitted from the sample. This unique tool comprised the basis for OCT.

OCT works in the ballistic regime. Like other ballistic imaging modalities, the measured photons are assumed to take straight paths. Its imaging depth is limited to ~1 mm, due to the rapid exponential attenuation of ballistic photons. But, it is able to provide μm-scale resolution imaging of tissues' scattering structure through coherence gating. In a highly scattering medium, the image quality degrades quickly after light penetrates several hundred μms because of multiple-scattering[9]. The multiple-scattered light can interfere with the reference light just like the single-scattered light.[10] It is also difficult to extract absorption information from OCT. Spectral information has previously been exploited to solve this problem at the cost of spatial resolution[11]. However, this method is susceptible to the spectral variation of the scattering coefficient μ_s, and is also unable to detect absorbers whose absorption coefficient μ_a does not change much in the source bandwidth.

In figure 1, we examine these two techniques in a big picture. In an imaging depth to resolution map, we noticed an obvious gap was left between DOT and OCT. An imaging technique is needed to image beyond 1 mm and provide sub-millimeter resolution. Optical CCT is initially designed to bridge this gap. It can work in the quasi-diffusive regime[12], where most photons are multiply scattered, however not totally diffused. We measure the time-resolved profiles of the reemitted light through multiple source-detection pairs. The side-scattered photons will also be collected. We also make full use of the multiple-scatter photons by adopting a DOT-like model-based reconstruction, thus can achieve deeper penetration than OCT. We also expect optical CCT will achieve finer spatial resolution than DOT, since we have finer temporal resolution and smaller source-detection separations. In addition, because the full inverse transient radiative transfer problem is solved during the reconstruction, it can potentially map all the optical properties.

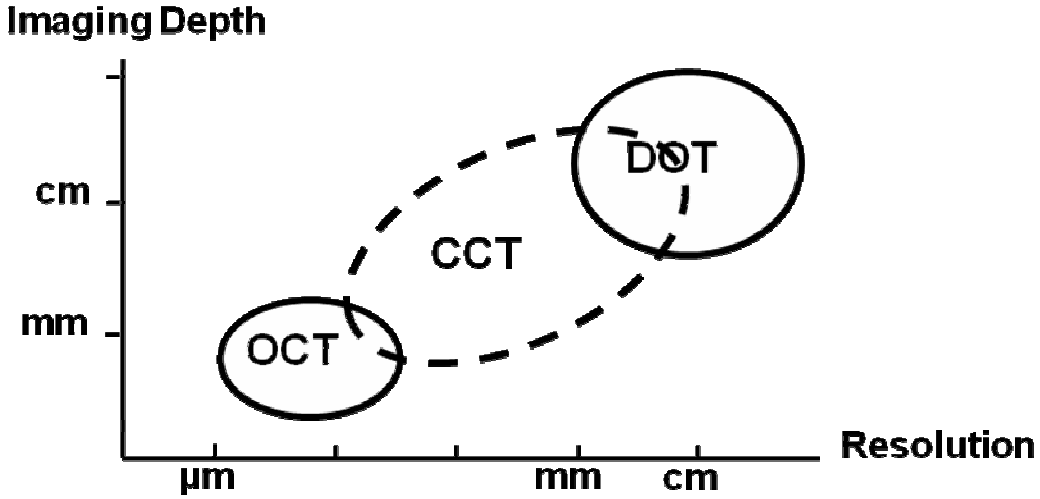

Figure 1 OCT, DOT and Optical CCT in a big picture.

2. METHODS

2.1 System setup

Our optical CCT system is shown in figure 2. It is based on a fiber-optic Mach-Zehnder interferometer. It is seeded by a broadband superluminescent diode (IPSDD0803, InPhenix, center wavelength λ_0=829 nm, bandwidth $\Delta\lambda$=36.4 nm). The achievable temporal resolution here is calculated to be 56 fs. This can be further reduced by increasing the source bandwidth. The cross-interference between light traveling through a fixed-length reference arm and the sample arm is recorded by a home-made spectrometer using a fast line-scan camera (Aviiva M2, Atmel, 12 bits, 2042 pixels). This spectral-domain scheme has been proved to be faster and more sensitive than its time-domain counterparts [13, 14] The polarization and dispersion differences between the two arms are carefully compensated for. The time-resolved profile of reemitted light is calculated from the recorded spectrum through Fourier transform. The illumination and collection optics are pre-aligned coaxially. Both can be scanned laterally (in the x-y plane) by a translation stage. This allows measurements through different source-detection pairs. This system can be easily parallelized, for example using a coherent fiber-bundle, in the future to increase the frame rate.

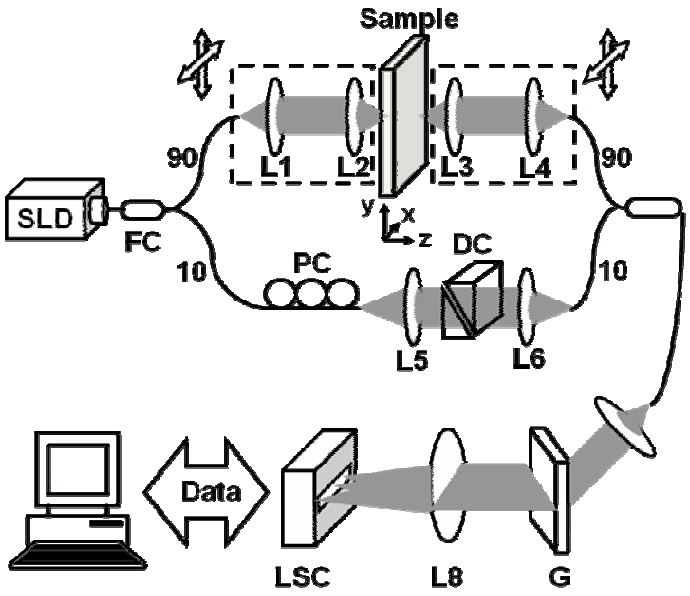

Figure 2 Experimental setup of optical coherence computed tomography. SLD: superluminescent diode; FC: fiber coupler; PC: polarization controller; DC: dispersion compensation; G: gratings; LSC: Line-scan camera; L1-8: lenses.

2.2 Image Reconstruction

Different from DOT, optical CCT can't use diffusion theory to model the underlying photon-migration problem, because the diffusion approximations are invalid for the quasi-diffusive regime. We must resort to the full transient radiative transport equation (RTE). As an initial demonstration of the concept of optical CCT, we aim to image the spatial distribution of absorption perturbation $\delta\mu_a$ here. Perturbations in scattering coefficient μ_s and the scattering phase function can be mapped by following similar procedures. From the RTE, the change in the measurement ΔT due to this absorption perturbation within the acceptance angle Ω_d is obtained under the first Born approximation as

$$\Delta T(\mathbf{r}_d, t_d) = -\int_{\Omega_d}\int_V\int_{4\pi}\int_t \hat{n}(\mathbf{r}_d)\cdot\hat{s}_d S(\mathbf{r}_s,\hat{s}_s,t_s)G(\mathbf{r},\hat{s},t;\mathbf{r}_s,\hat{s}_s,t_s)\delta\mu_a(\mathbf{r})G(\mathbf{r}_d,\hat{s}_d,t_d;\mathbf{r},\hat{s},t)dtd\Omega dVd\Omega_d$$

$$= -\int_V \delta\mu_a(\mathbf{r})\int_{\Omega_d}\int_{4\pi}\int_t \hat{n}(\mathbf{r}_d)\cdot\hat{s}_d S(\mathbf{r}_s,\hat{s}_s,t_s)G(\mathbf{r},\hat{s},t;\mathbf{r}_s,\hat{s}_s,t_s)G(\mathbf{r}_d,\hat{s}_d,t_d;\mathbf{r},\hat{s},t)dtd\Omega d\Omega_d dV$$

$$= -\int_V \delta\mu_a(\mathbf{r})J_0(\mathbf{r};\mathbf{r}_d,t_d)dV, \qquad (1)$$

where $\hat{n}$ is the inward normal of the detection surface. S is the source term. G is the Green's function solution for the transient RTE. The integration involving S and G can be merged into a single term J_0, which physically means the portion of measured signal that has been affected by the perturbation at $\mathbf{r}$. Eq. (1) represents a well-known linear inverse problem, which is widely studied in DOT. J_0, often referred to as the sensitivity function, is in practice calculated numerically through a time-resolved Monte Carlo method[15]. The experimental boundary condition is also included in our Monte Carlo simulation. The simultaneous iterative reconstruction technique (SIRT) is used to solve $\delta\mu_a$, since it in general yields better images than the regularized pseudo-inverse approach and the algebraic reconstruction technique. In real experiment, we used $M_0\Delta T / T_0$ instead of ΔT directly for inversion. This makes our reconstruction less susceptible to the boundary condition of the object. Here, T_0 and M_0 are the unperturbed measurements obtained through experiment and simulation, respectively. The integration time for recording a single spectrum was 1 ms. The signal from a single source-detection pair was the average based on 500 recorded spectra, where averaging alleviated the speckle noise.

2.3 Phantoms

The highly scattering tissue-mimicking phantom was constructed using aqueous suspension of 1-μm polystyrene microspheres. The optical properties calculated using the Mie theory were μ_s=113.6 cm^{-1} and scattering anisotropy g=0.90, whereas the absorption is negligible. The phantom used in our experiment was 2.6 mm thick, corresponding to ~30 scattering mean-free-paths. The absorbing target is 100-μm horse hair fibers. The hairs were immersed parallel to the y-axis inside the scattering medium described above.

3. RESULTS

3.1 Validation of experimental measurements

The time-resolved reemitted light measured by optical CCT was compared with the predictions from Monte Carlo simulation, a well accepted golden standard. Fig. 3(a) shows the measurements without absorbing objects with source position fixed at x=0 mm at different detection positions with lateral shift x ranging from -0.5 mm to 0.5 mm. The measurements at x=0.1 mm, 0.3mm, were compensated for the depth-dependent decay due to the finite spectral resolution and then were compared with the predictions from Monte Carlo simulation, as shown in Figs. 3(b) and (c). We can see they matched reasonably well.

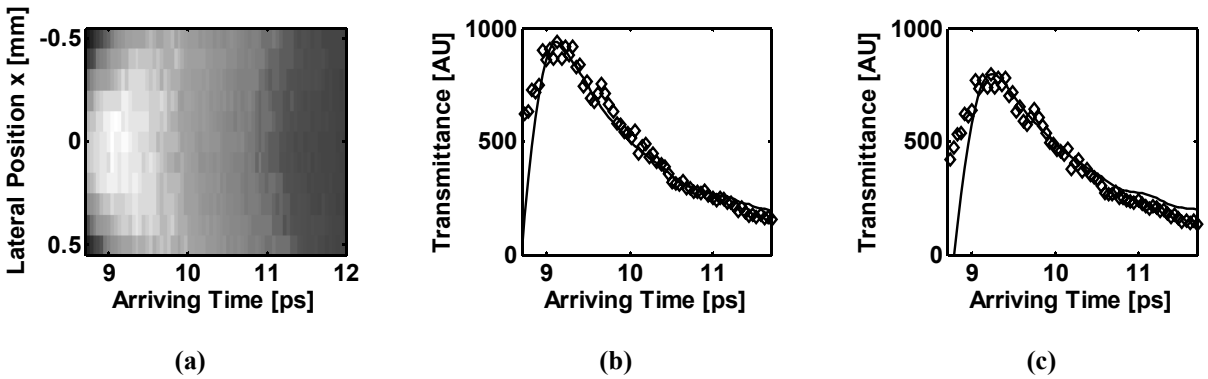

(a) (b) (c)

Figure 3 Experimental measurements by optical coherence computed tomography. (a) Measurements at different detection positions with lateral shift x=-0.5 mm to 0.5 mm for fixed source position at x=0 mm. Measurements at (b) x=0.1 mm and (c) x=0.3 mm is compared with the predictions from the Monte Carlo simulation. Solid lines: predication from Monte-Carlo simulation; Diamond: experimental measurements.

3.2 Image of a single absorber

To demonstrate the imaging capability, a hair fiber is inserted into the center of the high scattering medium. Data were collected at 11×11 source-detection pairs by optical CCT, which covered a 1-mm range along the x-axis. An image was reconstructed, as shown in figure 4(a). We faithfully imaged the hair, which was invisible to naked eyes, at the expected location. The cross lines through the center of the image were plotted in figure 4(b) and (c). The full width at half maximum (FWHM) of image was measured to be smaller than 200 μm at both x and z directions. Thus, after subtraction the diameter of the hair fiber, we estimate that the spatial resolution of our optical CCT system is better than 100 μm from the spatial spread under the assumption of a linear system.

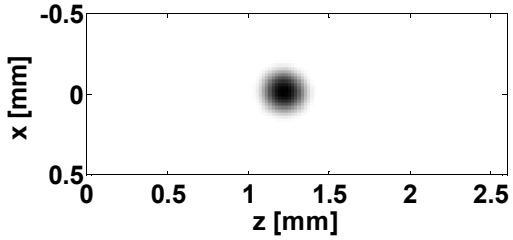

(a)

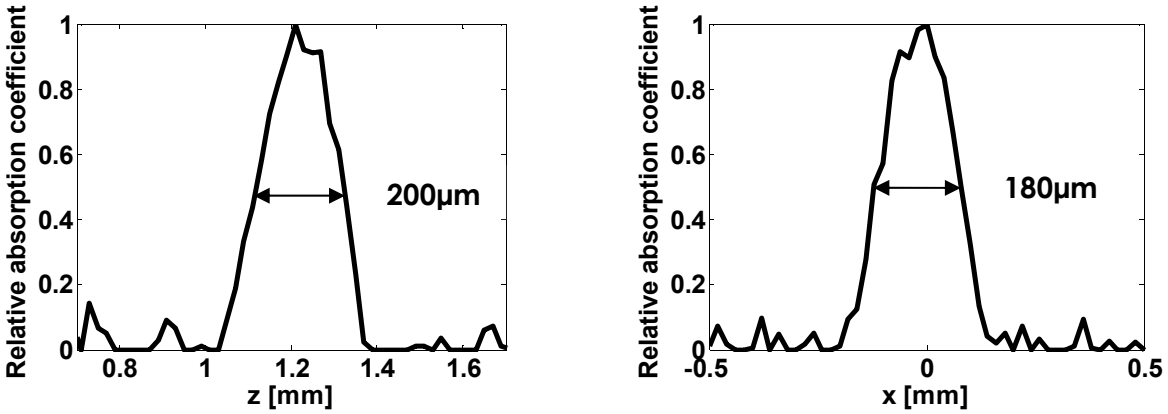

(b) (c)

Figure 4 (a)Optical CCT image of a single hair fiber. The image lines across the center of the image along (b) z-direction, and (c)x-direction.

3.3 One absorber at three different depths

The same hair fiber was then imaged at three different depths with a 0.5-mm separation. Figure 5 shows the three reconstructed images. The hair fiber was clearly identified at all three expected positions. This demonstrates that optical CCT can image absorbers at different depth and maintain the spatial resolution well throughout the imaging area.

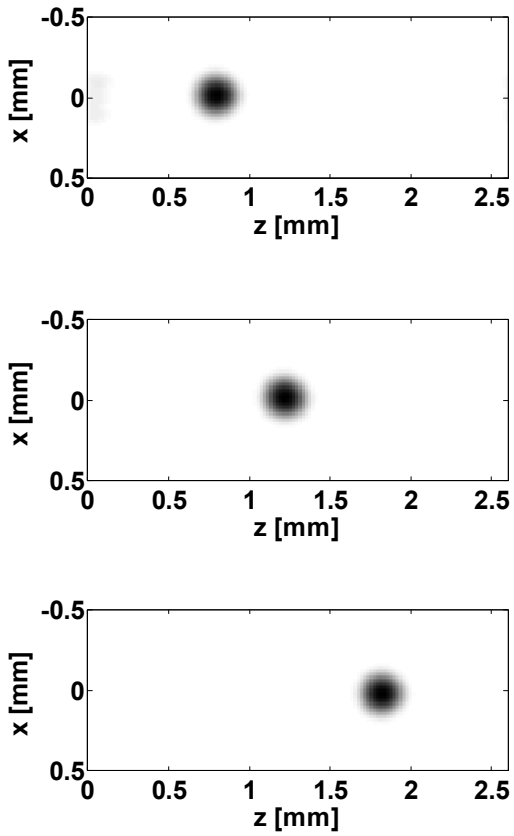

Figure 5 Optical CCT images of a 100-μm hair fiber at three different depths with 0.5-mm separation.

3.4 Multiple absorbers

Figure 6 shows the reconstructed image of two hair fibers in the scattering medium, with a 1.0-mm separation in the x-direction and 1.4-mm separation along z-direction. Transmitted light was measured at 21×21 source-detection pairs, which covered a 2-mm range along the x-axis. This demonstrates optical CCT is capable of mapping multiple absorption perturbations simultaneously.

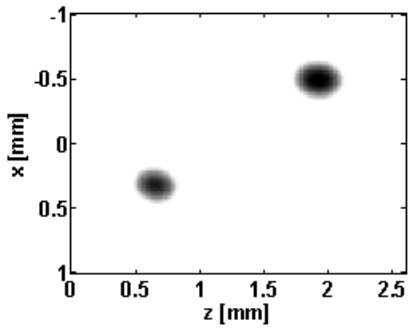

Figure 6 Optical CCT image of two hair fibers.

4. DISCUSSION

Previous development of imaging modalities for the quasi-diffusive regime is limited to laminar optical tomography (LOT)[16,17], which uses CW measurements. The image quality relies on proper regularization, and decays with depth. Since time-resolved measurements are adopted in optical CCT, the inverse problem is less ill-posed and the reconstruction is more robust. Optical CCT is also less sensitive to specular reflections than LOT, since the unwanted reflections fall outside the time gate.

Another unique advantage of optical CCT is that it can be scaled up to image thicker tissues by relaxing the temporal resolution, because the light detected at each time point increases with increasing time gate. Of course, this is done at the cost of spatial resolution. The scaled-up optical CCT is promising to provide a low-cost alternative to the current time-domain DOT. Detection of light after penetrating 1.5-cm chicken tissue was previously reported by relaxing the time gate to 900 fs[18] .

The linear perturbation assumption is known to fail when dealing with large perturbations, especially when they are located in close proximity. Previous prediction of spatial resolution will also fail because of this non-linearity. Under the circumstances, the non-linear image reconstruction problem needs to be solved through matching the prediction and the measurement using the forward model iteratively. The current Monte Carlo based forward model, although accurate, suffers from stochastic noise. To achieve acceptable smooth time-resolved simulation for the quasi-diffusive regime is extremely computation intensive. As a result, our current experiments are limited to imaging line objects (parallel with the y-axis) by using a sensitivity function integrated along the y-axis. Thus, a fast forward model is desirable for expanding the application of optical CCT. Recently, with the advance with time-resolved optical image techniques, researchers have started to develop various numerical solutions for solving the full transient RTE based on the discrete transfer method, the discrete ordinates method and finite volume method[19]. However, further studies are needed to clarify their applications in the content of biomedical optical imaging, especially for the quasi-diffusive regime. Their accuracy need to be tested against the Monte Carlo method, a well-accepted golden standard.

In conclusion, we demonstrated optical CCT as a 50-fs-time-resolved tomographic modality to provide tomographical images of absorption perturbations in the quasi-diffusive regime. This technique is important for high-resolution small animal imaging and dermal imaging beyond the penetration of OCT. A reflection-mode optical CCT, as well as its scaled-up version and proper fast forward model, is actively pursued in our group.

ACKNOWLEDGEMENTS

This work was supported in part by the National Institutes of Health grants R01 CA092415 and R01 CA106728.

REFERENCES

[1] Li L. and Wang L., "Optical coherence computed tomography," Appl. Phys. Lett., v91, 141107 (2007).
[2] Yodh A. and Boas D., [Biomedical Photonics Handbook], CRC Press, Boca Raton, Chapt. 21 (2003).
[3] Gibson A., Hebden J. and Arridge S., "Recent advances in diffuse optical imaging," Phys. Med. Biol., v50, R1-43 (2005).
[4] Huang D., Swanson E., Lin C., Schuman J., Stinson W., Chang W., Hee M., Flotte T., Gregory K., Puliafito C. and Fujimoto J., "Optical coherence tomography," Science, v254, 1178-1181 (1991).
[5] Bouma B. and Tearney G., [Handbook of Optical Coherence Tomography], Marcel Dekker, New York, (2002).
[6] Hebden J. and Delpy D., "Enhanced time-resolved imaging with a diffusion model of photon transport," Opt. Lett., v19, 311-313 (1994).
[7] Schmidt F., Fry M., Hillman E., Hebdan J. and Delpy D., "A 32-channel time-resolved instrument for medical optical tomography," Rev. Sci. Instrum., v71, 256-265 (2000).
[8] D'Andrea C., Comelli D., Pifferi A., Torricelli A., Valentini G. and Cubeddu R., "Time-resolved optical imaging through turbid media using a fast data acquisition system based on a gated CCD camera," J. Phys. D, v36, 1676-1681 (2003).
[9] Yadlowshy M., Schmitt J. and Bonner R., "Multiple scattering in optical coherence microscopy," Appl. Opt., v34, 5699-5707 (1995).
[10] Karamata B., Laubscher M., Leutenegger M., Bourquin S., Lasser T. and Lambelet P., "Multiple scattering in optical coherence tomography. I. Investigation and modeling," J. Opt. Soc. Am. A, v22, 1369-1379 (2005).
[11] Morgner U., Drexler W., Kärtner F., Li X., Pitris C., Ippen E. and Fujimoto J., "Spectroscopic optical coherence tomography," Opt. Lett., v25, 111-113 (2000).
[12] Wang L., and Wu H., [Biomedical Optics: Principles and Imaging], Wiley, New Jersey, Chapt. 5 (2007).
[13] deBoer J., Cense B., Park B., Pierce M., Tearney G. and Bouma B., "Improved signal-to-noise ratio in spectral-domain compared with time-domain optical coherence tomography," Opt. Lett., v28, 2067-2069 (2003).
[14] Leitgeb R., Hitzenberger C. and Fercher A., "Performance of fourier domain vs. time domain optical coherence tomography," Opt. Exp., v11, 889-894 (2003).
[15] Yao G. and Wang L., "Monte Carlo simulation of an optical coherence tomography signal in homogenous media," Phys. Med. Biol., v44, 2307-2320 (1999).
[16] Dunn A. and Boas D., "Transport-based image reconstruction in turbid media with small source-detector separations," Opt. Lett., v25, 1777-1779 (2000).
[17] Hillman E., Boas D., Dale M. and Dunn A., "Laminar optical tomography: demonstration of millimeter-scale depth-resolved imaging in turbid media," Opt. Lett., v29, 1650-1652 (2004).
[18] Hee M., Izatt J., Swanson E. and Fujimoto J., "Femtosecond transillumation tomography in thick tissues," Opt. Lett., v18, 1107-1109 (1993).
[19] Mishra S., Chugh P., Kumar P. and Mitra K., "Development and comparison of the DTM, the DOM and the FVM formulations for the short-pulse transport through a participating medium," International J. of Heat and Mass Transfer, v49, 1820-1832 (2006).